

Localization of chain dynamics in entangled polymer melts

M. G. Guenza*

Department of Chemistry and Biochemistry, and Institute of Theoretical Science, University of Oregon, Eugene, Oregon 97403, USA

(Received 1 April 2014; revised manuscript received 2 May 2014; published 27 May 2014)

The dynamics of polymer melts in both the unentangled and entangled regimes is described by a Langevin equation for the correlated motion of a group of chains, interacting through both intra- and inter-molecular potentials. Entanglements are represented by an intermolecular monomer-monomer confining potential that has no effect on short chains, while interpolymer interactions, responsible for correlated motion and subdiffusive center-of-mass dynamics, are represented by an intermolecular center-of-mass potential derived from the Ornstein-Zernike equation. This potential ensures that the liquid of phantom chains reproduces the compressibility and free energy of the real samples. For polyethylene melts the calculated dynamic structure factor is found to be in quantitative agreement with neutron spin echo experiments of polyethylene melts with chain lengths that span both the unentangled and the entangled regimes. The theory shows a progressive localization of the cooperative chain dynamics at the crossover from the unentangled to the entangled regime, in the spirit of the reptation model.

DOI: [10.1103/PhysRevE.89.052603](https://doi.org/10.1103/PhysRevE.89.052603)

PACS number(s): 83.80.Sg, 36.20.Fz, 82.35.Lr, 87.15.hg

I. INTRODUCTION

In the extended family of complex fluids, where dynamics develops on a wide range of time scales, polymer melts present unusual and unique properties. Diffusion and viscosity display different scaling exponents when the chain degree of polymerization, N , is increased beyond the characteristic value of N_e , which represents the statistical number of monomers delimited by entanglements in any given chain [1]. Entanglements are transient points of contact between chains, which constrain the extent of monomer fluctuations due to the impossibility of chains crossing each other (see, for example, Fig. 1). Going from unentangled to entangled dynamics, scaling of the diffusion coefficient varies from $D \propto N^{-1}$ to $D_e \propto N^{-2}$, and viscosity changes from $\eta \propto N$ to $\eta \propto N^{3.5}$, in apparent violation of the Stokes-Einstein law [2]. The different scaling exponents for the dynamics of short, unentangled chains ($N < N_e$) and long, entangled chains ($N > N_e$) indicates that the leading physical phenomena guiding chain motion in the two regimes are different [3]. However, the consistency of the structural and thermodynamic properties, as well as the smooth crossover of the dynamics at $N \approx N_e$, suggest that the same physical phenomena should be present in the dynamics of both unentangled and entangled polymers, while their relative relevance changes across the dynamical transition.

In this paper we present a theoretical approach, which describes, with quantitative precision, the dynamics of polymer melts across the dynamical transition. Despite the relevance of polymeric systems and the importance of properly modeling their dynamics in the liquid state, two theoretical approaches, formally incompatible, are commonly adopted for the dynamics in the two different regimes. For short chains, the dynamics is represented by a Langevin formalism, i.e., the Rouse approach, describing the time evolution of a chain of monomers in the mean field of the surrounding chains. For long chains the dynamics is described by the reptation model, which is a phenomenological mean-field approach describing the slithering of a polymer inside a “tube” formed by the

constraints of the interpenetrating entangled polymers [4]. Both approaches are successful in the regime where they apply, but each suffers from limitations, as extensively discussed in the literature [5–8].

For the reptation model, quantitative agreement with specific experiments has been achieved only at the expense of introducing physical and mathematical approximations that differ depending on the type of experiment against which the theory is tested. New approaches have been recently proposed to overcome this inconsistency, such as Likhtman’s slip-link model [9]. In general, the limitation of theoretical methods in the entangled regime is a consequence of their phenomenological nature, which requires the definition of a number of starting hypotheses on the nature of the dynamics involved.

II. A LANGEVIN APPROACH TO DYNAMICALLY HETEROGENEOUS, ENTANGLED POLYMER MELTS

Because polymer melts are viscous fluids at low Reynolds number, microscopic approaches to their dynamics are in the form of Langevin equations. Previous microscopic models of entangled polymer dynamics [10,11] have focused on the Langevin dynamics of a single chain, where entanglements enter as a perturbation to the unentangled friction, through the memory function.

The Langevin approach presented here describes the simultaneous dynamics of a group of n chains in a melt of either unentangled or entangled polymers, where entanglements are not accounted for in a perturbative way, but they enter the linearized part of the equation directly, through an effective intermonomer potential. This model is in the spirit of previous approaches, where entangled dynamics was evaluated by describing the simultaneous dynamics of a pair of entangled polymers [12,13].

The theory is general and applies to any liquid of linear polymer chains with variable monomeric structure. Due to its microscopic formalism, it can easily be implemented to treat block copolymers, polymer mixtures, and polymers with different degrees of branching. The approach is tested here to describe the dynamics of polyethylene melts across the

*mguenza@uoregon.edu

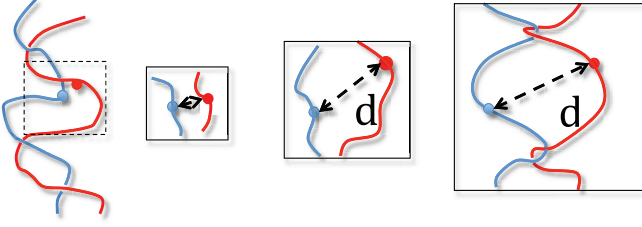


FIG. 1. (Color online) Model representation of a pair of monomers belonging to two entangled chains, which initially are in contact and then freely interdiffuse until they experience the constraint due to entanglements.

transition from unentangled to entangled, because for this polymer the most complete sets of experimental and simulation data are available in the literature [14].

A. The α parameter

The Langevin formalism presented here builds on the evidence that polymeric liquids are glass formers, and their dynamics is heterogeneous, with spatial regions of slow and fast motion [15]. The trademark of dynamical heterogeneities is an α parameter different from zero, with $\alpha(t) = (3/5)\{([r_m(t) - r_m(0)]^4)/([r_m(t) - r_m(0)]^2)^2\} - 1$, in the intermediate regime between ballistic and diffusive dynamics, where the dynamics is subdiffusive and the displacement is not Gaussian [16]. United atom molecular dynamics (UAMD) simulations of polyethylene melts, performed in the NVT ensemble, at the temperature and the density of the experimental data studied in this paper [17], and from the literature [18], show that the α parameter in all samples has consistent qualitative features. The dynamics (see Fig. 2) is heterogeneous up to the time of the crossover to Brownian dynamics. This is the time necessary for the dynamics to

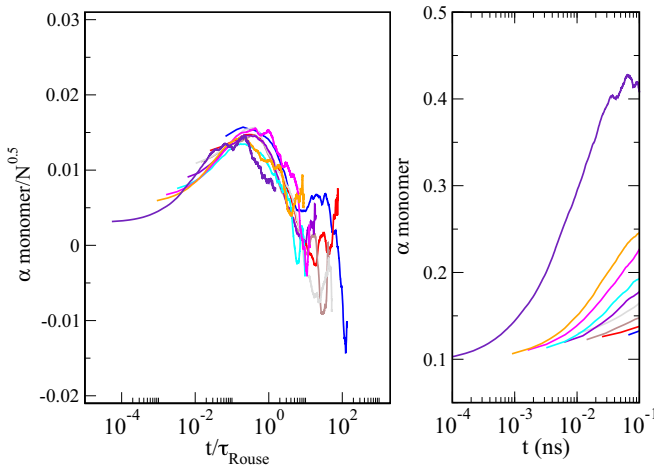


FIG. 2. (Color online) Left panel: Rescaled α parameter for polyethylene melts of increasing degree of polymerization ($N = 78, 100, 122, 142, 174, 224, 270, 320, 1000$, from the top to the bottom curve) from UAMD simulations. Data from simulations of Ref. [18]. Right panel: Same data as in the left panel, but without rescaling, and with increasing N from the bottom to the top curve.

become uncorrelated, where the decorrelation time is $\tau_{\text{Rouse}} \approx R_g^2/D$ for unentangled chains and $\tau_d \approx R_g^2/D_e$ for entangled.

From the analysis of computer simulations, we observe that at short times the degree of anomalous dynamics is independent of the degree of polymerization ($\alpha \approx 0.1$ for any N as shown in Fig. 2) because the monomer samples a local region of the liquid where the chain length does not yet affect the dynamics. In the intermediate regime α displays a maximum, which scales roughly as \sqrt{N} , for both unentangled and entangled melts, up to $N = 320$, while for the $N = 1000$ sample it is already difficult to define the maximum of the function from the simulations because of the lack of sampling in the long-time regime. The characteristic length scale of the dynamic heterogeneities is of the order of the molecular size R_g , because $\alpha = 0$ for $t \approx \tau_{\text{Rouse}}$ for unentangled chains, and $t \approx \tau_d$ for entangled chains.

B. A Langevin equation for entangled polymer dynamics

In a dynamically heterogeneous liquid, a set of coupled Langevin equations is derived from the Liouville equation for the dynamics of the liquid by projecting onto the coordinates of the slowly moving chains [19]. The time evolution of the space coordinates of a monomer i belonging to the polymer a , inside a group of the n polymers, follows the Langevin equation

$$\zeta \frac{d\mathbf{r}_a^{(i)}(t)}{dt} = -\frac{3k_B T}{l^2} \sum_{b=1}^N \mathbf{A}_{a,b} \mathbf{r}_b^{(i)}(t) - (n-1)K[r(t)]\mathbf{r}_a^{(i)}(t) + N^{-1} \sum_{j \neq i}^n \sum_{c=1}^N K[r(t)]\mathbf{r}_c^{(j)}(t) + \mathbf{F}_a^{(i)}(t), \quad (1)$$

where $\beta^{-1} = k_B T$ with k_B the Boltzmann constant and T the temperature in Kelvin, and ζ is the effective monomer friction coefficient. Here the matrix \mathbf{A} describes the intramolecular structure of a semiflexible finite-size polymer, and $K[r(t)]\mathbf{r}_a^{(i)}(t)$ is the intermolecular force:

$$K[r(t)]\mathbf{r}_a^{(i)}(t) \approx \frac{1}{\beta} \frac{\partial}{\partial \mathbf{r}_a^{(i)}(t)} \ln[g(r,t)] \quad (2)$$

where $g(r,t)$ is the probability of finding a pair of monomers belonging to different, but dynamically correlated chains at a relative distance r at time t . The set of coupled equations is solved by first applying a similarity transform which isolates relative and collective dynamics of the n chains undergoing slow cooperative motion, and then decoupling the equations by Fourier transforming into relative, ξ_p , and collective, χ_p , normal modes by diagonalization of the single-chain intramolecular matrix \mathbf{A} with eigenvectors $Q_{i,p}$ and eigenvalues λ_p [19]. The approach reduces to the Rouse equation in the limit of a single, infinitely long, totally flexible phantom chain, which is not directly interacting with the surrounding chains.

The zeroth normal-mode coupled equations of motion describe the relative and collective dynamics of the center of mass (c.m.) of the n correlated chains, which depend on the effective intermolecular force acting between any pair of polymers in the melt. The related potential is present in both unentangled and entangled polymer liquids, and results from the propagation

through the liquid of the intermolecular monomer-monomer interactions, i.e., Lennard-Jones potential. The analytical form of the intermolecular potential that acts between the c.m. of pairs of phantom chains in a polymer liquid has been recently derived [20]. This potential ensures the consistency of both structural and thermodynamic properties of the polymer liquid, described either at the monomer level in a molecular dynamics simulation or as a liquid of interacting phantom chains, as in the Langevin, or Rouse, approach. The potential does not vanish even in the limit of infinitely long chains [20].

As these intermolecular interactions enter the dynamics at the level of the c.m., they correspond to an effective potential in the $p = 0$ mode representation. Because the potential is a function of the instantaneous distance between the c.m. of a pair of chains, which evolves in time as polymers interdiffuse, at each fixed time interval the equation of motion is solved self-consistently to recover the intermolecular distance entering the potential. Once self-consistency is ensured for the $p = 0$ mode at a given time interval, the local dynamics is optimized by enforcing self-consistency in the intermolecular *monomer* distance, i.e., for the $p \neq 0$ modes.

At the monomer level, inside the group of n slowly moving macromolecules, the dynamics is affected not only by the local conformational barriers, which enter the matrix \mathbf{A} , expressed in the semiflexibility parameter, but also by the impossibility of chains to cross each other. For a monomer in a chain segment limited by entanglements, fluctuations are confined to a given volume, which is defined by the maximum relative distance, d , that two monomers, belonging to a pair of entangled chains, can move relative to each other before experiencing constraint in their dynamics (see Fig. 1).

C. Intermolecular monomer potential due to entanglements

For a pair of interpenetrating chains, two monomers that at initial time are in contact, freely interdiffuse until they reach a relative distance at which they start to experience the constraint due to entanglements. We name this average relative distance d . The effective force acting between these two monomers is the derivative of the time dependent potential of mean force, expressed as a function of the conditional probability, $g(r, t)$, that if two monomers are in contact at time zero they will be at a relative distance $r(t)$ at time t . More specifically, for $r(t) \leq d$ the potential is $V_m[r(t)] = 0$, while for $r(t) > d$ the effective potential is $V_m[r(t)] \propto -\beta^{-1} \rho_{\text{ent}} \langle \ln g[r(t)] \rangle$, where the interaction is weighted by the number density of entanglements in the given volume, $\rho_{\text{ent}} = \rho/N_e$. The intermonomer interaction is averaged over the Gaussian distribution of monomers in the segment between entanglements, and results in an effective potential, for $r(t) > d$, $V_m[r(t)] \approx \rho_{\text{ent}} k_B T \{ \exp[-(r(t) - d)^2/d^2] + \exp[-[r(t) - 2d]^2/d^2] \}$. The direct comparison of the theoretical dynamic structure factor with neutron spin echo (NSE) experiments defines the numerical value of the parameter d , which is found to agree with the average statistical distance between two entanglements, $d \approx \sqrt{N_e} l$.

The constraint due to entanglements is applied to all samples, unentangled and entangled, independent of the degree of polymerization, but has no effect on the dynamics of unentangled chains because short chains relax before they sample the entanglement constraints. The correlation times,

in the relative and collective mode descriptions, are given by

$$\frac{t}{\tau_{\xi, p}(t)} = \frac{t}{\tau_{\chi, p}(t)} = \frac{k_s \lambda_p t}{\zeta} + \frac{(n-1)}{\zeta} \int_0^t K[r(t')] dt', \quad (3)$$

and $k_s = 3k_B T/l^2$. For $r(t) \leq d$, $K[r(t')] = 0$, and the unentangled dynamics is recovered. For long chains this corresponds to the short-time regime, where the polymer has not yet experienced the presence of entanglements, $t \leq d^2/D$.

III. TESTING THE THEORY AGAINST NEUTRON SPIN ECHO EXPERIMENTS

The theory is directly compared with NSE experiments of the intermediate scattering function, $S(\mathbf{q}, t) = N^{-1} \sum_{i,j=1}^N \langle \exp\{i\mathbf{q} \cdot [\mathbf{r}_i(t) - \mathbf{r}_j(0)]\} \rangle$, defined in Kubo's cumulant expansion as [21,22]

$$S(\mathbf{q}, t) \approx \frac{1}{N} \sum_{i,j=1}^N e^{-(q^2/6) f(q^2) \langle [\mathbf{r}_i(t) - \mathbf{r}_j(0)]^2 \rangle}, \quad (4)$$

with $f(q^2) = 1 - q^2 \alpha(t) \langle [\mathbf{r}_m(t) - \mathbf{r}_m(0)]^2 \rangle / 12 + O(q^4)$ and where $\alpha(t)$ is the α parameter described above.

The theoretically calculated intermediate scattering function shows quantitative agreement with experimental data of NSE [14,23], for samples of polyethylene melts with increasing degree of polymerization, spanning a range from $N = 36$, which is unentangled, to the entangled regime with the degree of polymerization of $N = 1692$, where $N \approx 13N_e$. Figure 3 displays two samples at the crossover between unentangled and entangled dynamics, while the samples in Fig. 4 are in the entangled regime.

Experimental parameters that enter the theory are the temperature $T = 509$ K, density $\rho = 0.733$ g/cm³, the segment length $l = 1.53$ Å, and the effective stiffness parameter $g = 0.785$, which reproduces the radius of gyration of the polyethylene samples. In the case of short, unentangled, polymer chains the monomer friction coefficient ζ is calculated

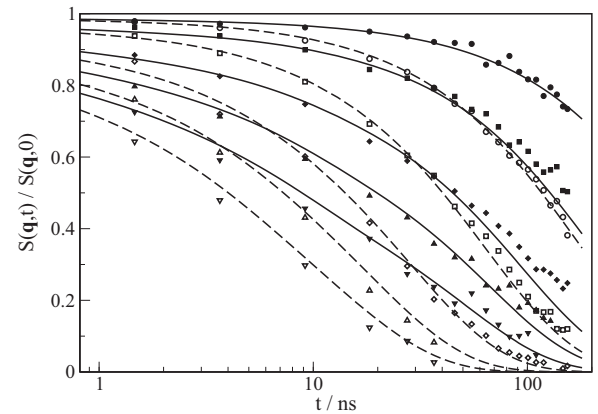


FIG. 3. Comparison between theoretical (lines) and experimental (symbols) values of the normalized incoherent intermediate scattering function for polyethylene with $N = 192$ (dashed lines) and $N = 377$ (full lines) at increasing wave vector $q = 0.3$ (circle), 0.5 (square), 0.77 (diamond), 0.96 (triangle up), 1.15 (triangle down).

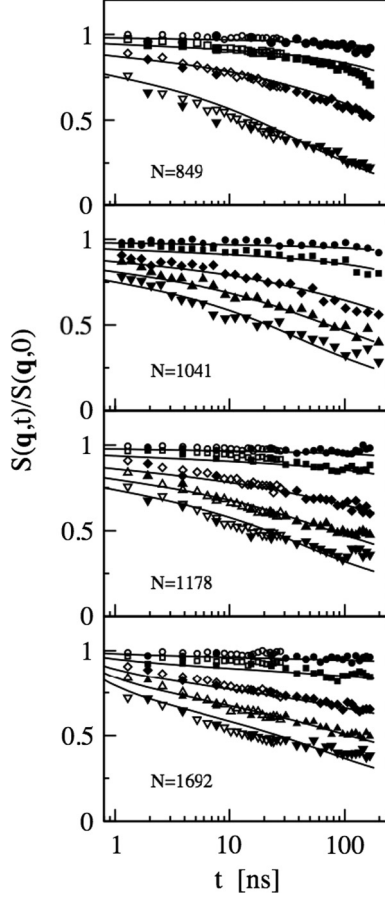


FIG. 4. Comparison between theoretical (lines) and experimental (symbols) normalized incoherent intermediate scattering functions for samples of increasing degree of polymerization, and increasing wave vector $q = 0.3$ (circle), 0.5 (square), 0.77 (diamond), 0.96 (triangle up), 1.15 (triangle down). Symbols are for samples measured at two different neutron wavelengths, $\lambda = 8 \text{ \AA}$ (filled symbols) and $\lambda = 15 \text{ \AA}$ (open symbols) [24].

from the NSE data of diffusion coefficient measured in the long-time regime where the dynamics is Fickian, as $\zeta = k_B T / (ND)$ [14]. For entangled polymer melts, the NSE data do not reach the diffusive regime, and the friction is calculated by optimization of the agreement between theory and experiments. Values of the friction calculated with the described procedure are consistent with those obtained from coarse-grained simulations of polyethylene melts properly rescaled [25], with the diffusion coefficient measured in independent experiments [26,27], and recover the scaling behavior of $D \propto N^{-2}$ typical of the entangled systems, as shown in the left panel of Fig. 5.

Two nontrivial parameters are optimized by direct comparison of the theory with experiments. The first is the distance that two monomers can move relative to each other before they experience the constraint due to the presence of entanglements. The value of d is found to be identical for all the entangled samples, and consistent with $d = \sqrt{N_e} l$ for $l = 1.53 \text{ \AA}$ and $N_e = 130$ for polyethylene.

The second is the number of interpenetrating chains, n , statistically included in the volume spanned by the radius

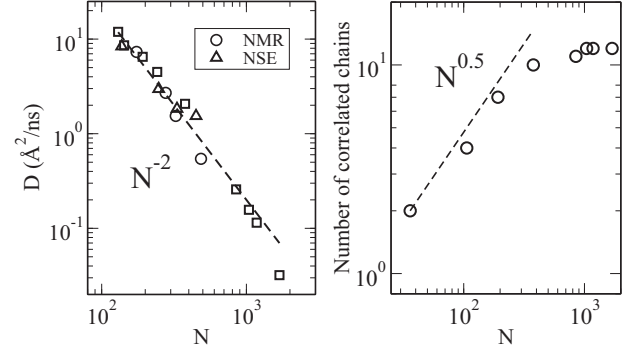


FIG. 5. Optimized parameters. Left panel: Diffusion coefficient of entangled samples, calculated using the numerically optimized friction coefficient (squares) as a function of the degree of chain polymerization, and compared with NMR data from Ref. [26] (circles), and NSE data from Ref. [27] (triangle). Right panel: Numerically optimized number of macromolecules undergoing cooperative dynamics as a function of the molecular degree of polymerization. Crossover to entangled dynamics is at $N_e = 130$.

of gyration, $R_g^3 \propto N^{1.5} l^3$, of a chain of N monomers. This number, $n \approx \rho \sqrt{N} l_{\text{eff}}^3$, is expected to increase with increasing polymer stiffness and with increasing density. The optimized value of n (see Fig. 5, right panel) shows agreement with the predicted scaling with N in the unentangled regime [14]. However, at the crossover from unentangled to entangled dynamics ($N \approx N_e$) and in the entangled region, the number of dynamically correlated chains stays constant at $n = 12$, which is the number of chains comprised in the volume defined by the length between two entanglements. This indicates that, in this time window, the dynamics of entangled samples is dominated by the presence of entanglements, which limits the cooperative dynamics of the polymers to a region that is defined by the characteristic length scale of an entangled strand.

IV. CONCLUSIONS

The dynamics of polymer melts from the unentangled to the fully entangled regimes is well described by a Langevin equation for the relative motion of a subensemble of interacting polymers. The theory is microscopic and specific to the polymer considered and to the thermodynamic conditions of the sample. No assumptions are made about specific mechanisms of relaxation; instead the dynamics is represented as the time evolution of the position coordinates of monomeric units in a group of polymer chains, which interact through intermolecular potentials, including the effect of entanglements. Numerical values of the input parameters, the monomer friction coefficient, the entanglement length, and the number of interpenetrating chains, are in agreement with the values expected, based on physical considerations. The equation represents well the anomalous dynamics emerging from the presence of the group of dynamically correlated molecules, and describes the coupling between entanglements and anomalous dynamics in entangled polymer melts. The model ensures thermodynamic consistency with experiments, while it accounts for the semiflexibility, finite size, and monomer structure of a given polymer.

ACKNOWLEDGMENTS

Computational resources were provided by Trestles through the XSEDE project supported by NSF. We acknowledge support from the National Science Foundation under

Grant No. DMR-0804145, and partial support under Grant No. PHY11-25915. We thank Gary Grest and Vlasios Mavrantzas for kindly sharing simulation trajectories, and James McCarty for performing UAMD simulations.

-
- [1] M. Rubinstein and E. Helfand, *J. Chem. Phys.* **82**, 2477 (1985); C. Tzoumanekas and D. N. Theodorou, *Macromolecules (Washington, DC, US)* **39**, 4592 (2006); R. S. Hoy, K. Foteinopoulou, and M. Kroger, *Phys. Rev. E* **80**, 031803 (2009).
- [2] M. Doi and S. F. Edwards, *The Theory of Polymer Dynamics* (Oxford University Press, New York, 1986).
- [3] R. H. Colby, L. J. Fetters, and W. W. Graessley, *Macromolecules (Washington, DC, US)* **20**, 2226 (1987); T. P. Lodge, *Phys. Rev. Lett.* **83**, 3218 (1999); S.-Q. Wang, *J. Pol. Sci.: Pol. Phys.* **41**, 1589 (2003).
- [4] P. G. de Gennes and L. Léger, *Ann. Rev. Phys. Chem.* **33**, 49 (1982).
- [5] A. E. Likhtman, *J. Non-Newtonian Fluid Mech.* **157**, 158 (2009).
- [6] T. C. B. McLeish, *Adv. Phys.* **51**, 1379 (2002); T. Lodge, N. Rotstein, and S. Prager, *Adv. Chem. Phys.* **79**, 1 (1990).
- [7] B. Wang, J. Guan, S. M. Anthony, S. C. Bae, K. S. Schweizer, and S. Granick, *Phys. Rev. Lett.* **104**, 118301 (2010).
- [8] J. X. Hou, C. Svaneborg, R. Everaers, and G. S. Grest, *Phys. Rev. Lett.* **105**, 068301 (2010).
- [9] A. E. Likhtman, *Macromolecules (Washington, DC, US)* **38**, 6128 (2005).
- [10] W. Hess, *Macromolecules (Washington, DC, US)* **21**, 2620 (1988).
- [11] K. S. Schweizer, *J. Chem. Phys.* **91**, 5802 (2010).
- [12] J. des Cloizeaux, *J. Phys. (Paris)* **3**, 61 (1993).
- [13] G. Szamel, *Phys. Rev. Lett.* **70**, 3744 (1993).
- [14] M. Zamponi, A. Wischniewski, M. Monkenbusch, L. Willner, D. Richter, P. Falus, B. Farago, and M. G. Guenza, *J. Phys. Chem. B* **112**, 16220 (2008).
- [15] K. Ngai, *Relaxation and Diffusion in Complex Systems* (Springer, New York, 2011).
- [16] X. Di and G. B. McKenna, *J. Chem. Phys.* **138**, 12A530 (2013).
- [17] J. McCarty, A. Clark, I. Y. Lyubimov, and M. G. Guenza, *Macromolecules (Washington, DC, US)* **45**, 8482 (2012).
- [18] N. Ch. Karayiannis, V. G. Mavrantzas, and D. N. Theodorou, *Phys. Rev. Lett.* **88**, 105503 (2002); N. Ch. Karayiannis, A. E. Giannousaki, V. G. Mavrantzas, and D. N. Theodorou, *J. Chem. Phys.* **117**, 5465 (2002); N. Ch. Karayiannis and V. G. Mavrantzas, *Macromolecules (Washington, DC, US)* **38**, 8583 (2005); P. S. Stephanou, C. Baig, and V. G. Mavrantzas, *Soft Matter* **7**, 380 (2011).
- [19] M. Guenza, *Phys. Rev. Lett.* **88**, 025901 (2001); *Macromolecules (Washington, DC, US)* **35**, 2714 (2002); *J. Chem. Phys.* **119**, 7568 (2003); *J. Phys.: Condens. Matter* **19**, 205115 (2007).
- [20] A. J. Clark, J. McCarty, I. Y. Lyubimov, and M. G. Guenza, *Phys. Rev. Lett.* **109**, 168301 (2012).
- [21] R. Kubo, *J. Phys. Soc. Jpn.* **17**, 1100 (1962).
- [22] M. Brodeck, F. Alvarez, A. Arbe, F. Juranyi, T. Unruh, O. Holderer, J. Colmenero, and D. Richter, *J. Chem. Phys.* **130**, 094908 (2009).
- [23] A. Wischniewski, M. Monkenbusch, L. Willner, D. Richter, A. E. Likhtman, T. C. B. McLeish, and B. Farago, *Phys. Rev. Lett.* **88**, 058301 (2002).
- [24] P. Schleger, B. Farago, C. Lartigue, A. Kollmar, and D. Richter, *Phys. Rev. Lett.* **81**, 124 (1998).
- [25] I. Y. Lyubimov and M. G. Guenza, *Phys. Rev. E* **84**, 031801 (2011).
- [26] D. S. Pearson, G. Ver Strate, E. von Meerwall, and F. C. Schilling, *Macromolecules (Washington, DC, US)* **20**, 1133 (1987); D. S. Pearson, L. J. Fetters, W. W. Graessley, G. Ver Strate, and E. von Meerwall, *ibid.* **27**, 711 (1994).
- [27] D. Richter, L. Willner, A. Zirkel, B. Farago, L. J. Fetters, and J. S. Huang, *Phys. Rev. Lett.* **71**, 4158 (1993).